Determination of Convergence Rates Across the Ventura Basin, Southern California, Using GPS and Historical Triangulation

Andrea Donnellan,
Bradford H. Hager,
and Shawn Larsen

Abstract

Comparison of angles from historical triangulation observations dating as far back as 1932 with Global Positions System (GPS) measurements taken in 1987 indicates that rapid convergence may be taking place on decade timescales in the central and eastern part of the Ventura basin, an east-west trending trough bounded by thrust faults. Changes in angles over this time were analyzed using Prescott's modified Frank's method and in terms of a model which assumes that the regions to the north and south of the basin are rigid blocks undergoing relative motion. For the two block model, inversion of the observed angle changes over the last 28 years for the relative motion vector leads to north-south convergence across the basin of 30 ± 5 mm/yr, with a left lateral component of 10 ± 1 mm/yr in the Fillmore-Santa Paula area in the central part of the basin. The modified Frank's method yields strain rates of $\sim$2microrad/yr in both the east and central parts of the basin for measurements spanning the 1971 San Fernando earthquake. Assuming no east-west strain yeilds north-south compression of $\sim3.5\pm.2$ cm/yr. Comparison of triangulation data prior to the earthquake shows no strain outside the margin of error.

The convergence rates determined by geodetic techniques are consistent with geologic observations in the area. Such large geodetic deformation rates, with no apparent near-surface creep on the major thrust faults in the area, can be understood if these faults become subhorizontal at relatively shallow depths and if the subhorizontal portions of the faults are creeping. An alternative explanation of the large displacement rates might be that the pumping of oil in the vicinity of the benchmarks caused large horizontal motions, although it is unlikely that meter scale horizontal motions are due to oil withdrawal. We are evaluating these and other hypotheses at present to better constrain the tectonics of this active region.

Seismotectonic Map

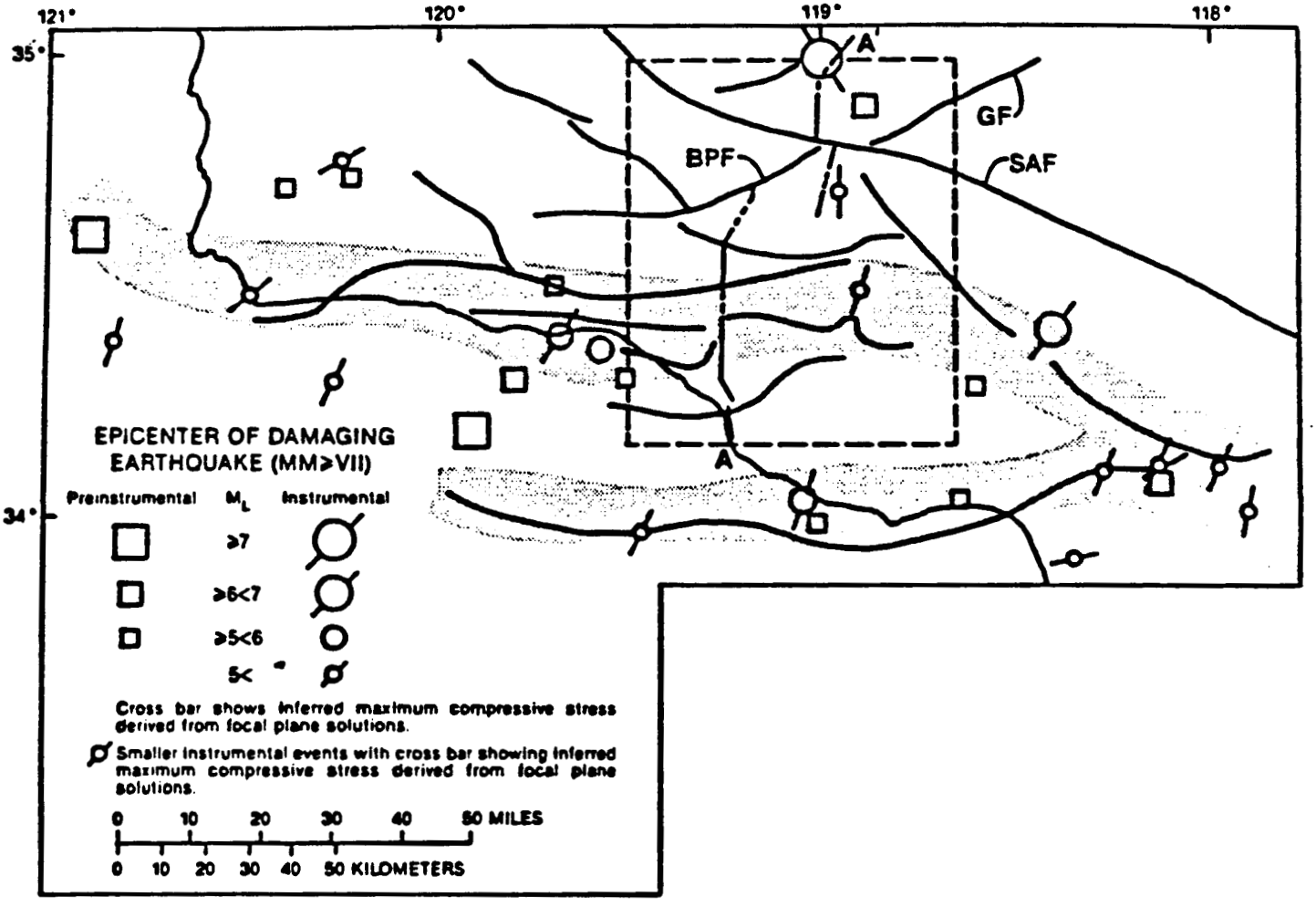

Generalized seismotectonic map for western and central Transverse Ranges. Stippled areas are zones of high seismicity characterized by compressive (north-south) focal mechanisms, east-west trending quaternary folds, thrust and reverse faults, and steep range fronts. (From Namson and Davis, in press.)

Location Map

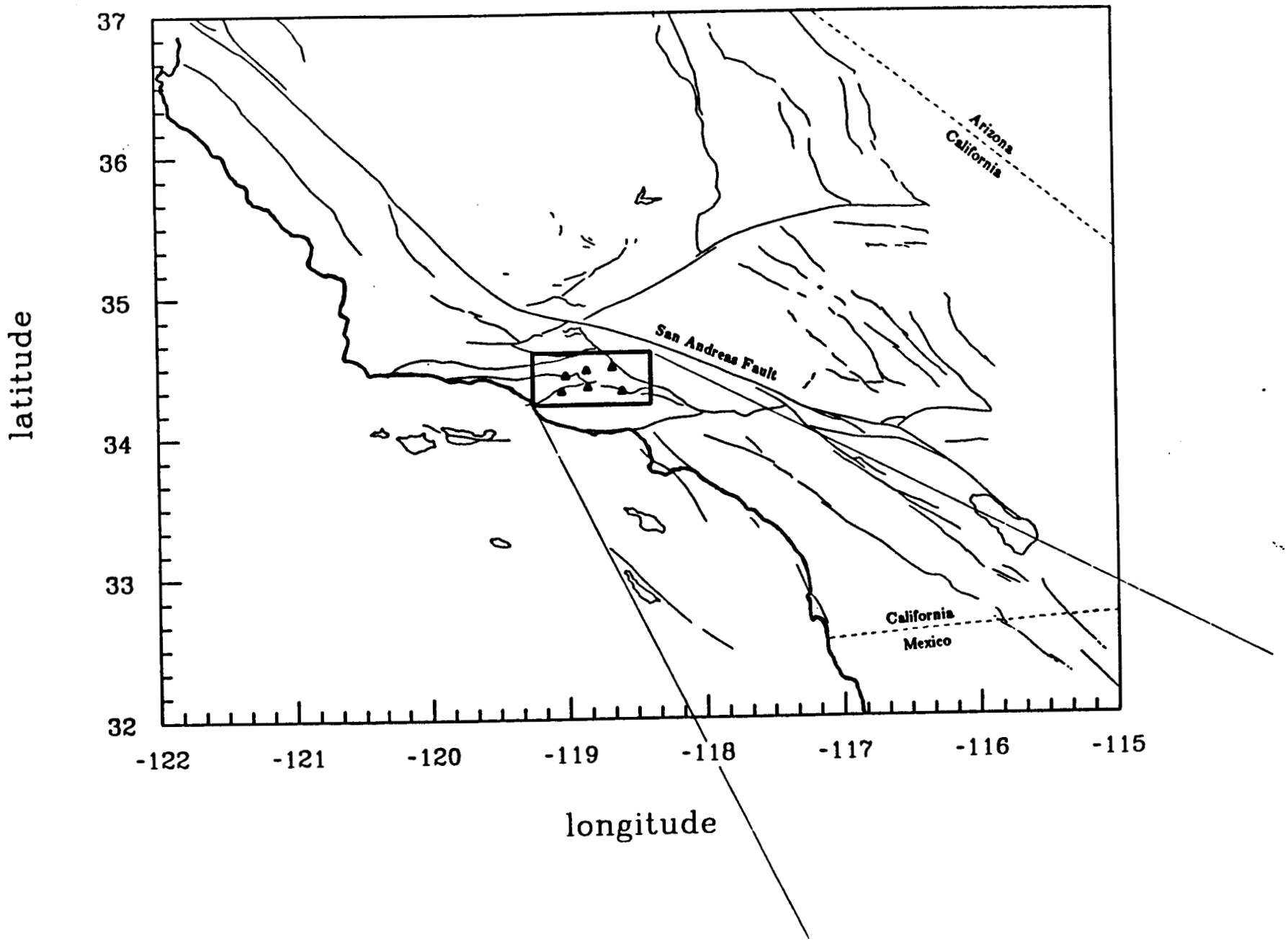

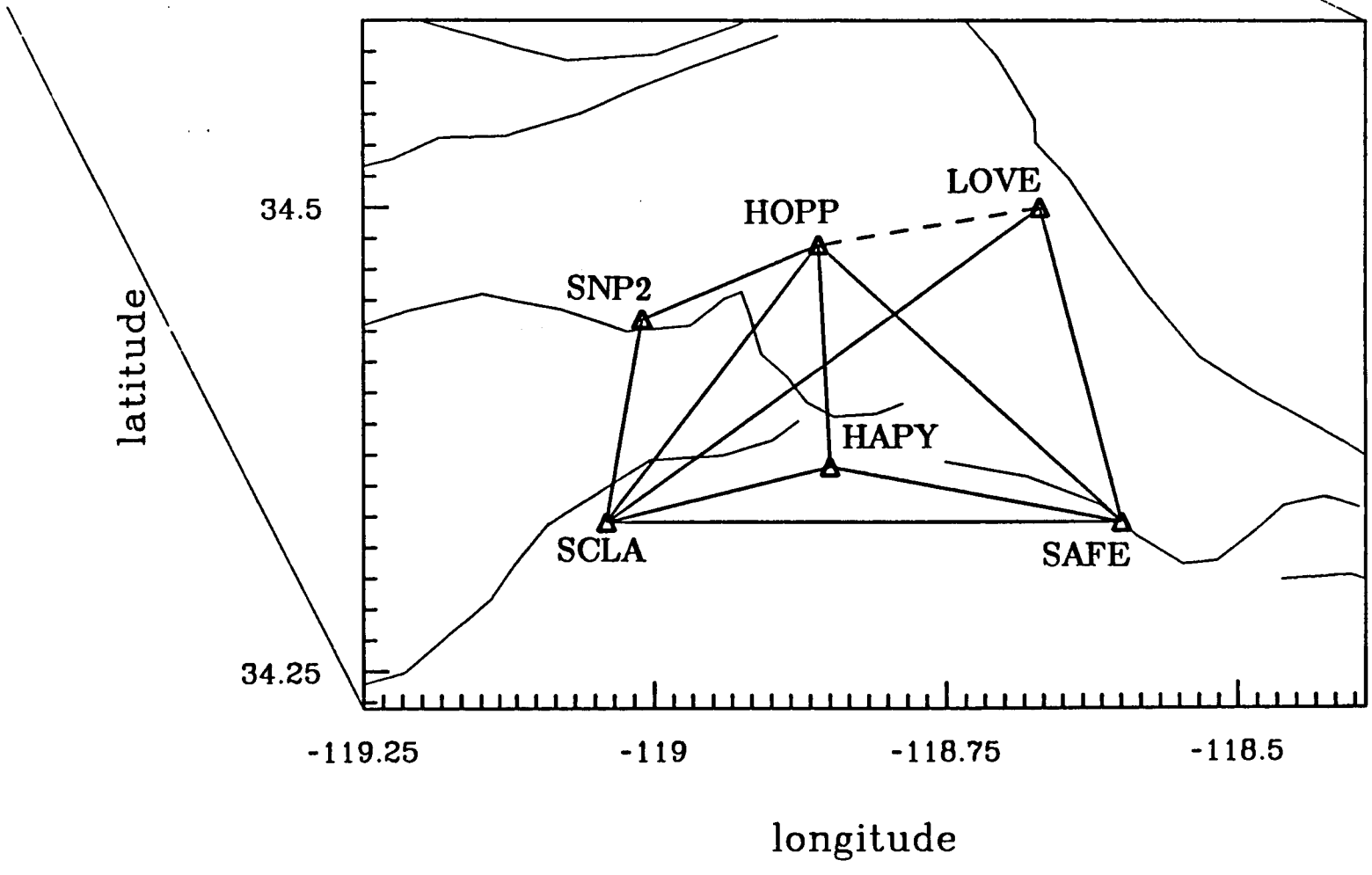
Ventura Basin Network
34.5
34.25
latitude
LOVE
HOPP
SNP2
HAPY
SCLA
SAFE
-119.25
-119
-118.75
-118.5
longitude

Various Strain Ellipses

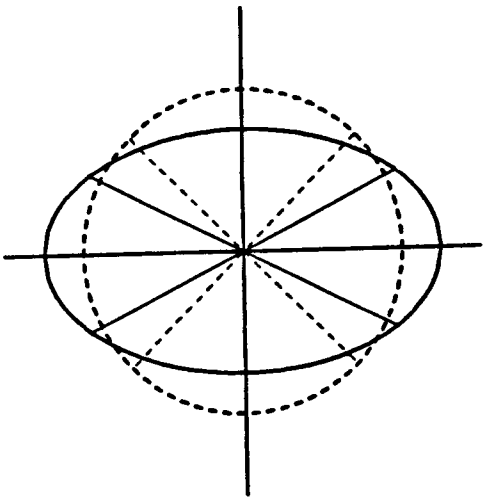

Case 1: e11+e22=0

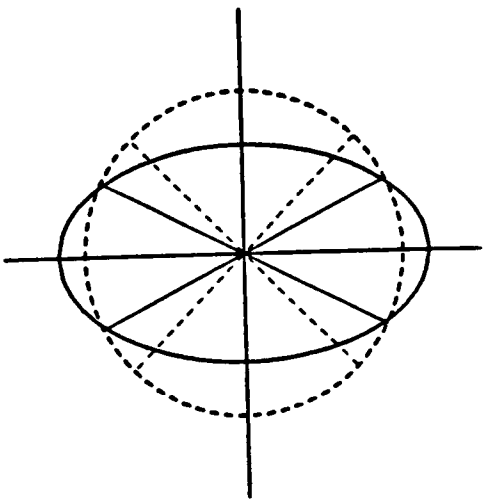

Case 2: e11+2e22=0

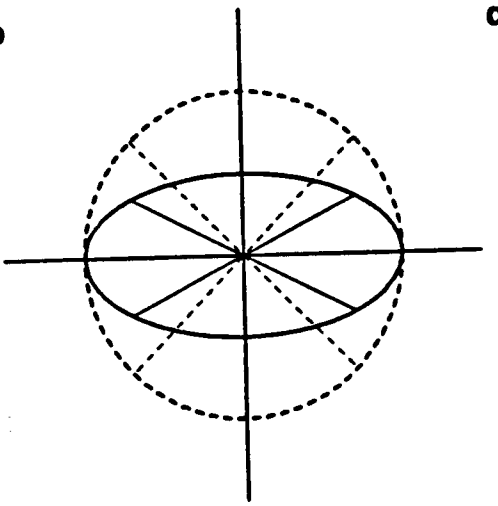

Case 3: e22=0

For triangulation surveys only shear strain components $\gamma 1$ and $\gamma 2$ can be determined, where $\gamma 1$=(e11-e22) and $\gamma 2$=(e12+e21). For the same γ (angular change) the values of e11 and e22 are not unique as shown above. Convergence rates cannot, therefore, be uniquely determined from triangulation surveys, although a maximum rate can be obtained.

Fillmore Area

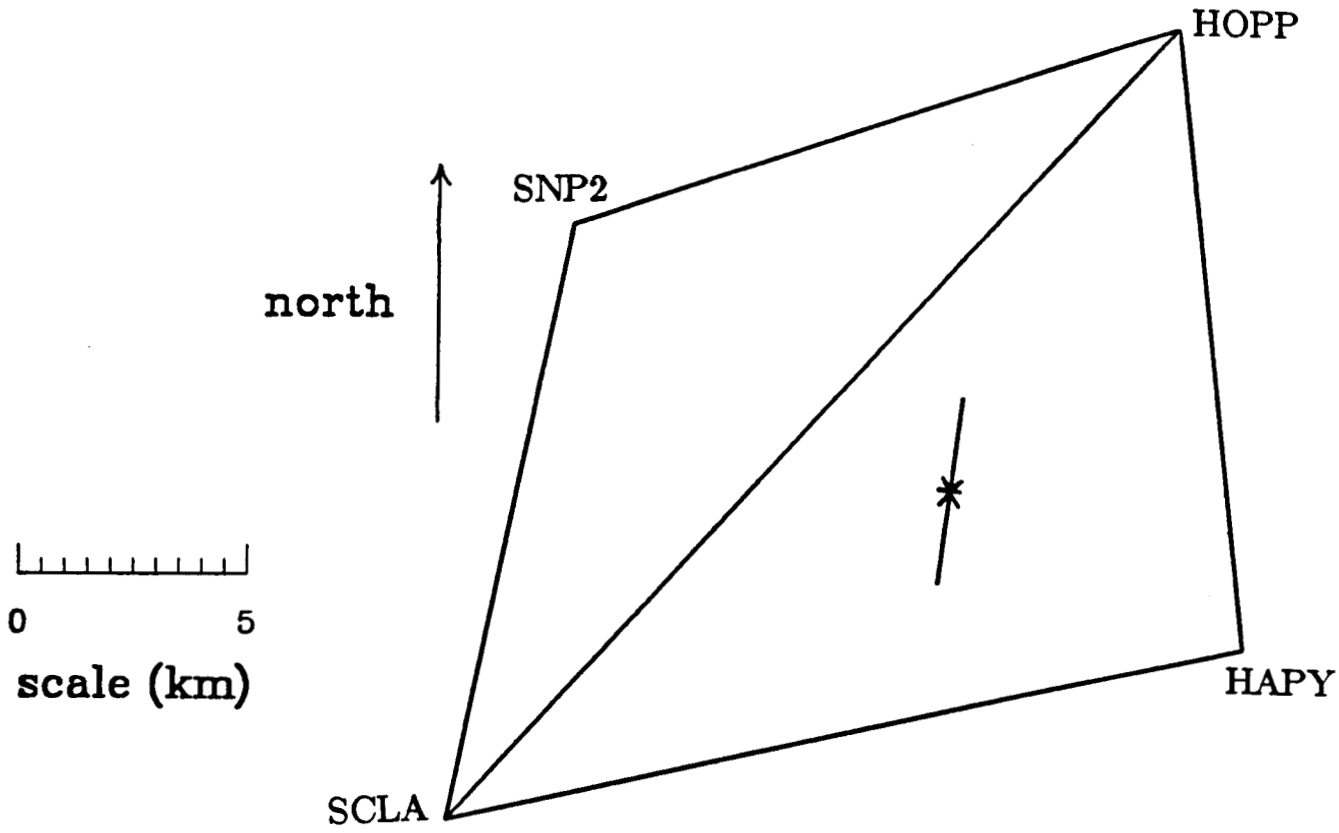

$\gamma 1 = \quad 2.28 \pm 0.31 \quad \mu$rad/year

$\gamma 2 = -0.62 \pm 0.14 \quad \mu$rad/year

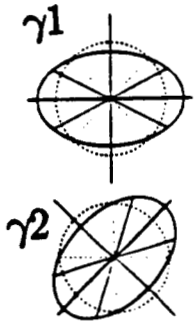

azimuth of maximum shear: $52° \pm 3°$

azimuth of maximum compression: $7° \pm 3°$

baseline=15 km

		e11	rate (cm/yr)
case1	(e11+e22=0):	1.091×10^{-6}	1.77 ± 0.2 cm/yr
case2	(e11+2e22=0):	1.455×10^{-6}	2.36 ± 0.2 cm/yr
case3	(e22=0):	2.183×10^{-6}	3.54 ± 0.2 cm/yr

Residual Plots--Fillmore Area

Fit of model to data for the western part of the network. Points represent the observed angles and the line represents the predicted change in angle versus time for that station. Although each station is plotted separately, the calculations use the data from all four stations in the area.

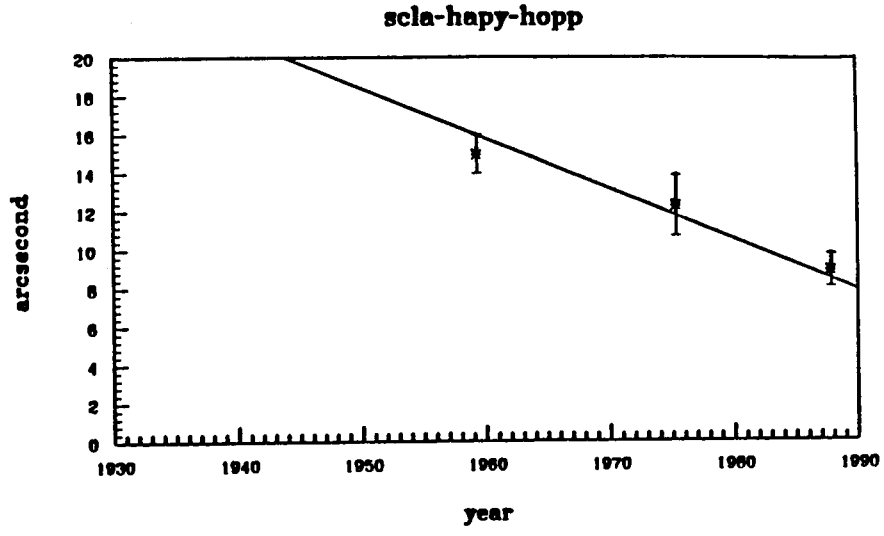

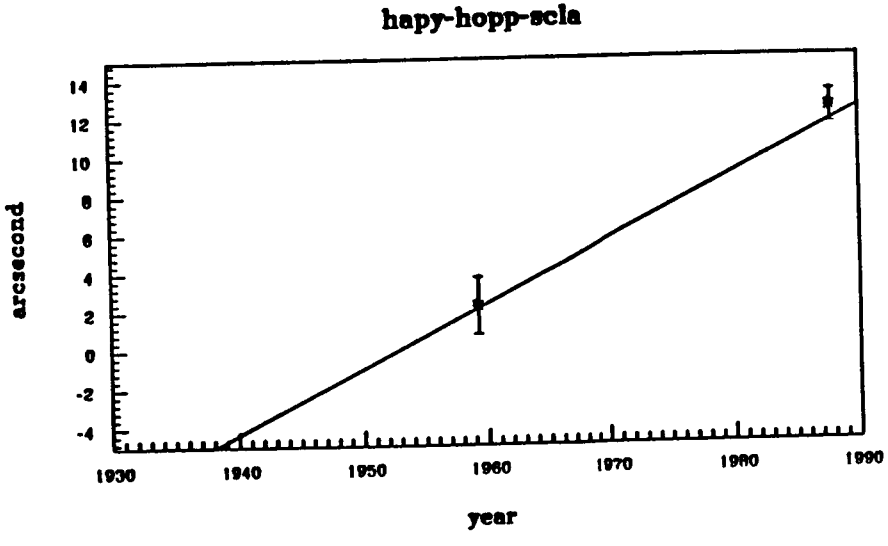

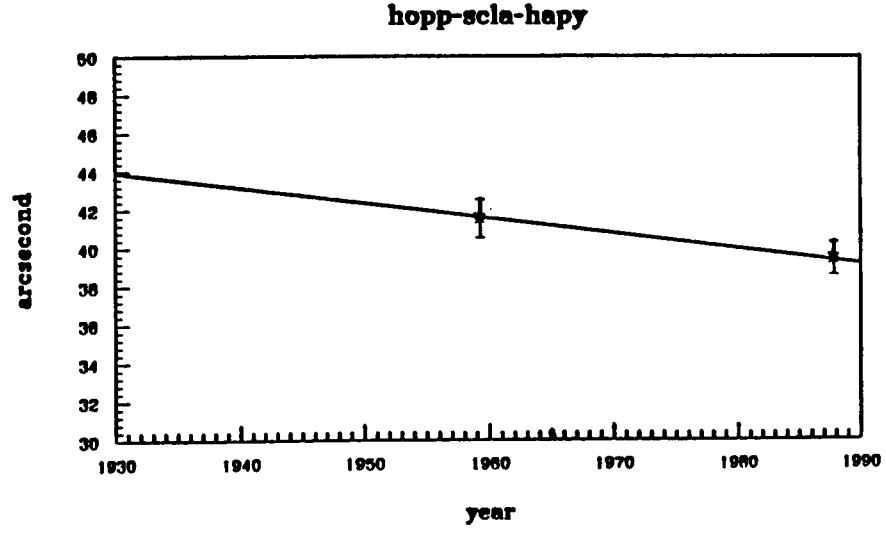

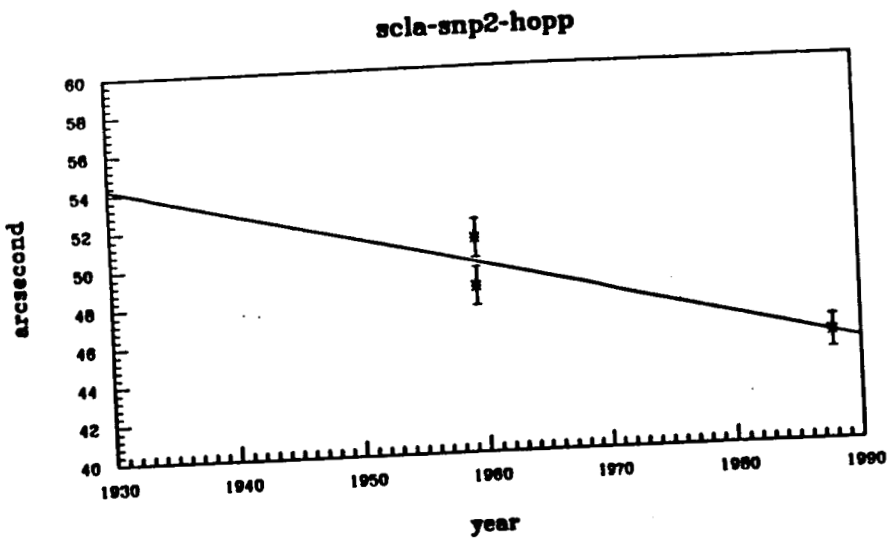
scla-snp2-hopp
arcsecond
60
58
56
54
52
50
48
46
44
42
40
1930
1940
1950
1960
1970
1980
1990
year

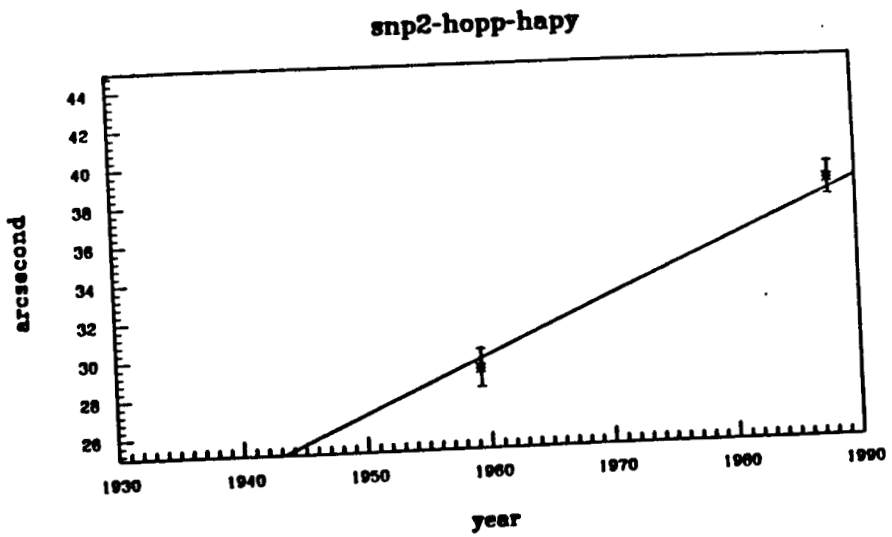
snp2-hopp-hapy
arcsecond
44
42
40
38
36
34
32
30
28
26
1930
1940
1950
1960
1970
1980
1990
year

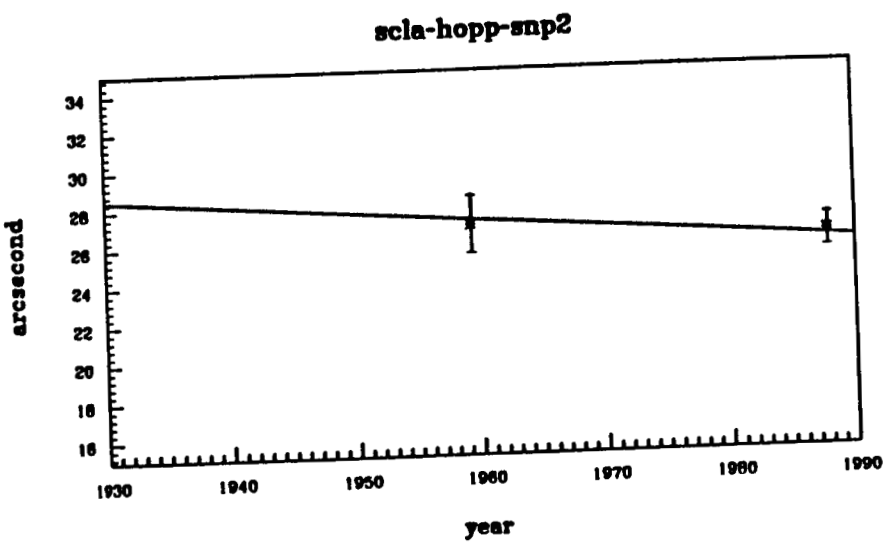
scla-hopp-snp2
arcsecond
34
32
30
28
26
24
22
20
18
16
1930
1940
1950
1960
1970
1980
1990
year

San Fernando Area*

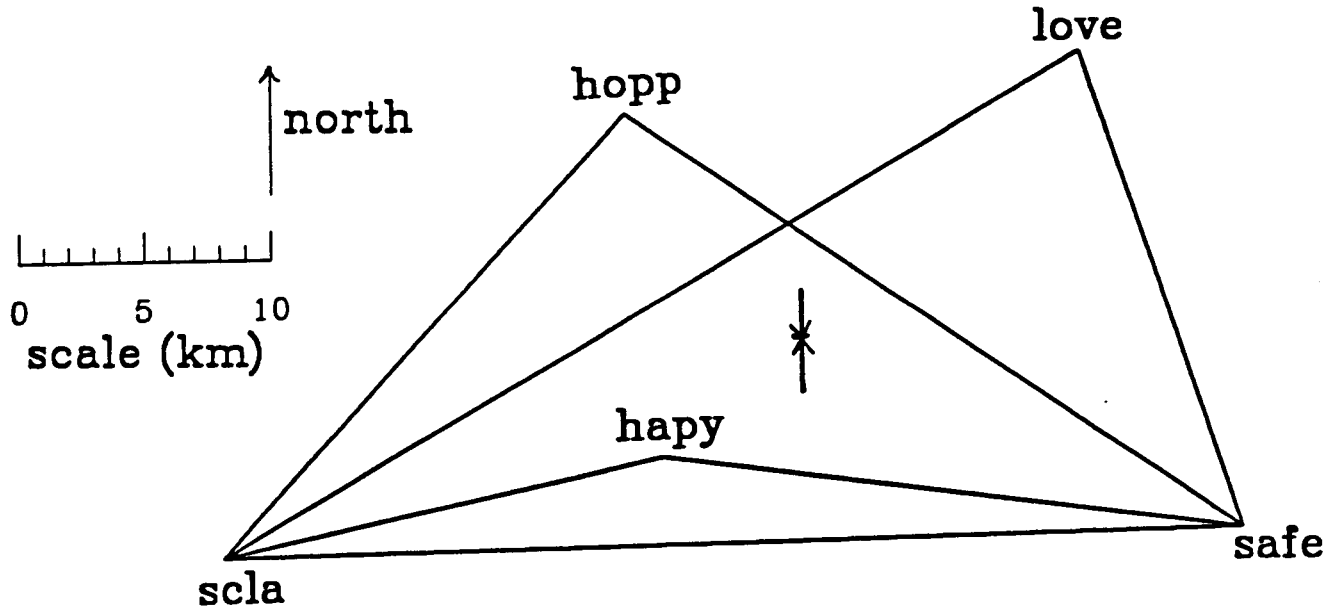

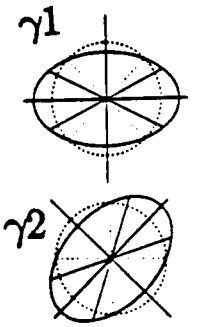

$\gamma 1 = \quad 2.18 \pm 0.12 \quad \mu$rad/year

$\gamma 2 = 0.04 \pm 0.15 \quad \mu$rad/year

azimuth of maximum shear: $44° \pm 2°$

azimuth of maximum compression: $-1° \pm 2°$

baseline=18 km

		e11	rate (cm/yr)
case2	(e11+e22=0):	1.091×10^{-6}	1.97 ± 0.2 cm/yr
case3	(e11+2e22=0):	1.455×10^{-6}	2.62 ± 0.2 cm/yr
case1	(e22=0):	2.183×10^{-6}	3.93 ± 0.2 cm/yr

* values are for most recent measurements

Residual Plots--San Fernando Area

Fit of model to data for the eastern part of the network. These stations lie near the location of the 1971 San Fernando earthquake. Two models were fit to this data set. The dashed lines represent a fit to all data preceding the 1971 earthquake. The solid lines show a fit to those data which fall nearest to and span the 1971 event. These three plots are a selection of 9 such plots for the area showing the best and worst fits.

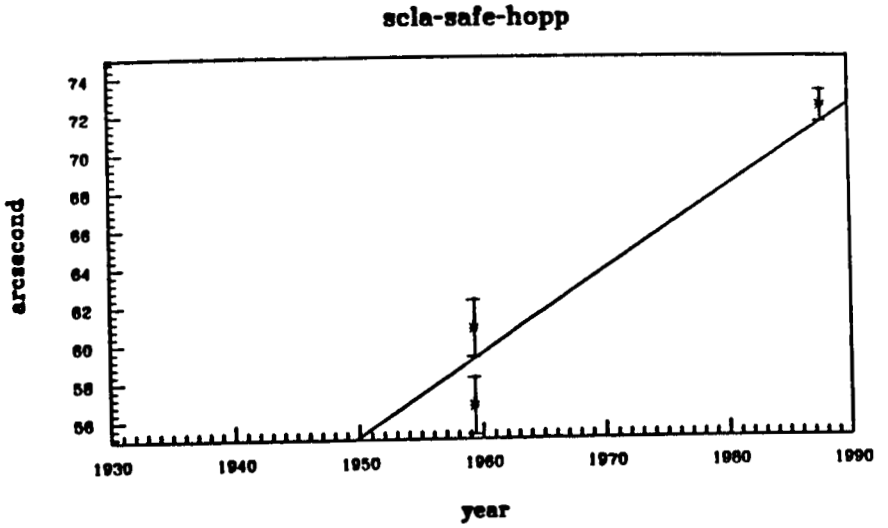

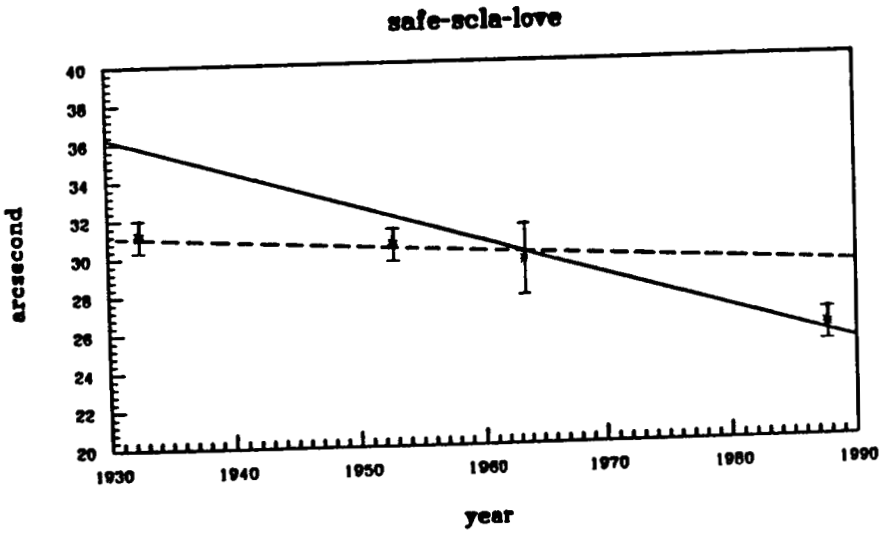

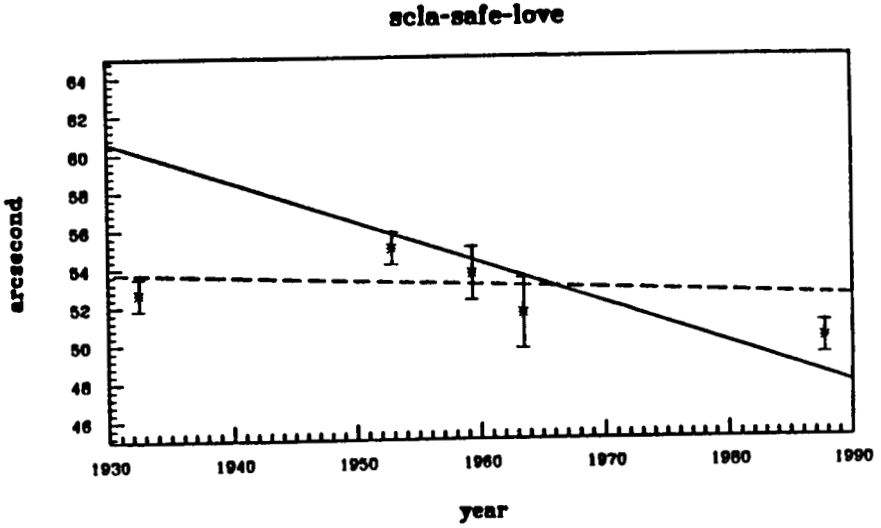

Supporting Information

1. **Focal mechanisms**
   - → horizontal on average
   - → indicate north-south compression

2. **Local geology**
   - → north and south dipping thrusts
   - → folds with east-west trending axes

3. **Inferred from the local geology**
   - → 2.3 cm/yr average convergence rate across basin in last 200 k.y. (Yeats, 1983).

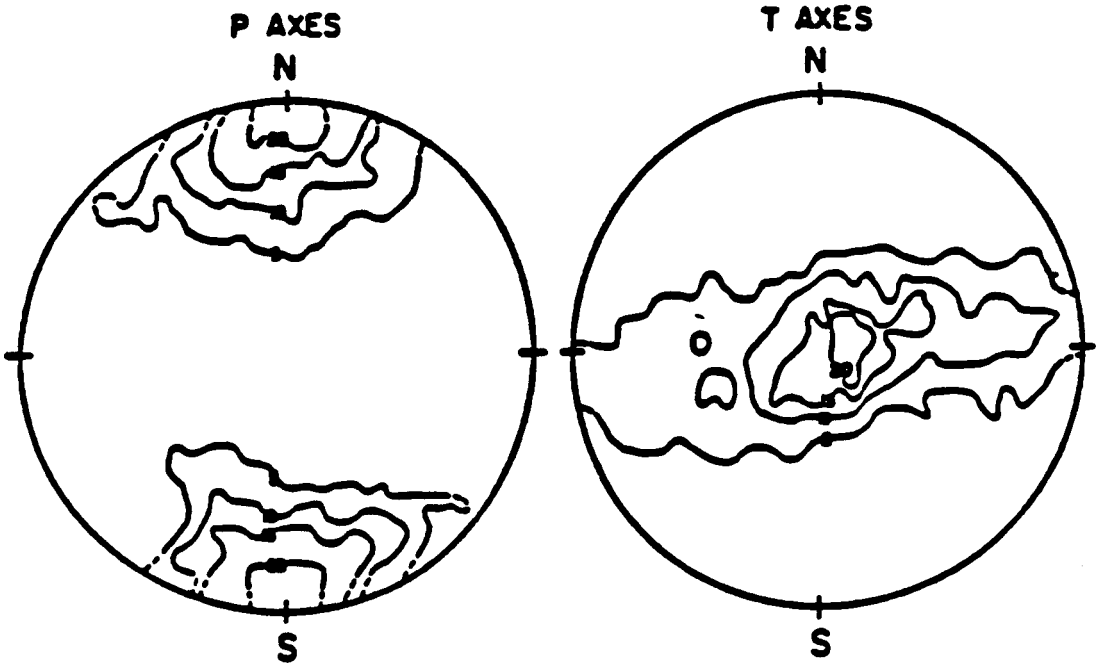

Contours of P and T axis locations from focal mechanisms for earthquakes in the Central Transverse Ranges. In Webb and Kanamori (1985), from Pechmann (1983).

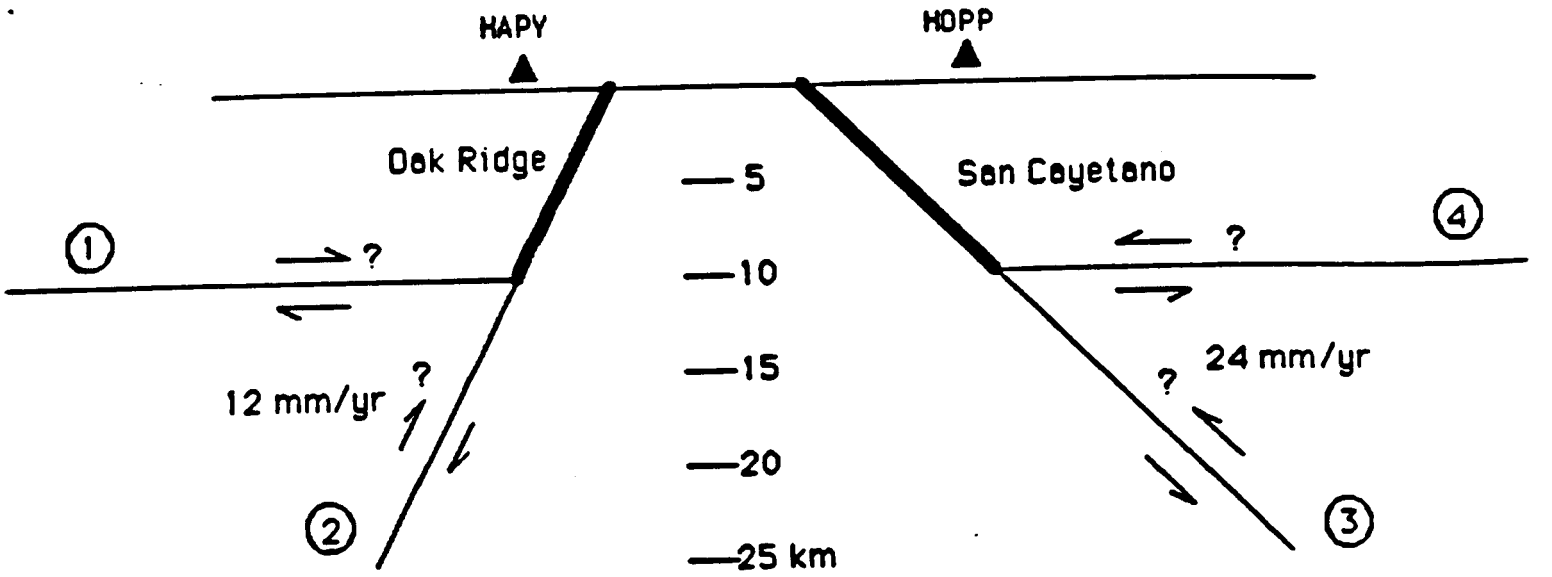

Fault	HAPY north	HAPY up	HOPP north	HOPP up	conver-gence	HAPY rel. uplift
1	5.3	3.8	3.7	1.4	1.6	2.4
2	0.7	1.1	0.8	0.7	-0.1	0.4
3	-7.4	2.8	-10.6	7.6	3.2	-4.8
4	-4.6	9.8	-3.0	3.8	1.6	6.0
1+3	-2.1	6.4	-6.9	9.0	4.8	-2.4
2+4	-3.9	10.9	-2.2	4.5	1.5	6.4

A cartoon of two end member models for creep at depth on the faults bounding the Ventura Basin. The heavy lines represent locked portions of the faults, while possibilities for slipping planes are shown with thin lines. Locations of two historical triangulation and GPS measurements which have been compared are indicated. The deformation at the surface depends strongly on whether the creeping fault segments are subhorizontal or steeply dipping, as well as on the depth of the creeping segment of the fault. Displacement rates (in mm/yr) at these sites for slip on the various model faults are given.

Comparison of NGS and Bernese Software

Results presented are for one day of data. The data for the stations listed below have been reduced using both the NGS and Bernese software packages.

Baseline Differences (NGS-Bernese)

Baseline	NGS	Bernese	Difference
hapy - pver	79642.449	79642.434	.015m
hopp - pver	91915.891	91915.877	.021m
scla - pver	87253.674	87253.657	.017m
hapy - hopp	13378.545	13378.544	.001m
hapy - scla	17762.397	17762.395	.002m
hopp - scla	23239.286	23239.278	.008m

Angle Differences (NGS-Bernese)

Angle	NGS	Bernese	Difference
ha-ho-sc	49 34' 12.28"	49 34' 11.63"	0.65"
ho-sc-ha	34 55' 39.43"	34 55' 39.37"	0.06"
sc-ha-ho	95 30' 8.88"	95 30' 9.46"	0.58"